Structure of amorphous carbon films deposited on Ni nanoparticles under ultrahigh vacuum at room temperature

Koji Asaka and Yahachi Saito

Department of Quantum Engineering, Graduate School of Engineering, Nagoya University, Furo-cho, Chikusa-ku, Nagoya 464-8603, Japan

Abstract

We present transmission electron microscopy (TEM) and Raman spectroscopy of amorphous carbon (a-C) films deposited on clean surfaces of nickel (Ni) nanoparticles at room temperature. In the Raman spectrum measured from the a-C film on the Ni nanoparticles, the broad peaks of the D and G modes appeared at 1388 and 1582 cm^{-1}, respectively. The high-resolution images and the corresponding filtered inverse fast Fourier transformed images of the a-C film on the individual Ni nanoparticles showed that the a-C film only around the Ni nanoparticles formed disordered graphitic layers, similar in structure to carbon black, without heat treatment. The present observation suggests that spontaneous graphitization of a-C on the clean surfaces of the Ni nanoparticles occurs at room temperature.

Keywords: graphitization of amorphous carbon, transmission electron microscopy, Raman spectroscopy.

1. Introduction

Graphene has attracted a lot of interest as a two-dimensional material with its extraordinary properties, such as high carrier mobility, thermal and electrical conductivity, and mechanical strength,[1-5] which have led to many applications.[6,7] As one of approaches to producing graphene, a method by annealing a solid carbon source, such as a polymer film or an amorphous carbon (a-C) film, on a metal catalyst substrate, e.g., a nickele (Ni) substrate, was proposed.[8-12] The metal-catalyzed graphitization of the a-C film can be utilized to produce large-area graphene and improve the quality of graphene, which lead to the development of graphene-based devices. The mechanism of the metal-catalyzed graphitization of the a-C film reportedly involves the dissolution of carbon into the catalytic metal at temperatures above 873 K and the precipitation of carbon as graphene on the surface from the solid solution in process of cooling. From this perspective, it is considered that the initial state of the metal surfaces serving as a reaction field, especially, the cleanliness influences the formation of graphene. For previous studies on the metal-catalyzed graphitization of the a-C film, it seems that the structure of as-deposited a-C films on the clean surfaces of the catalytic metals has not been studied in detail. In this report, we used the clean surfaces of Ni nanoparticles as the catalysts and investigated the structure of the as-deposited a-C films on these Ni nanoparticles by transmission electron microscopy (TEM) and Raman spectroscopy.

2. Experimental

Specimens were prepared by electron beam deposition in an ultrahigh vacuum chamber with a base pressure of less than 3×10^{-7} Pa. Sodium chloride (NaCl) (001) surfaces cleaved in air were used as substrates. Pure Ni (99.99 %) and carbon rods (99.998%) were used as evaporation sources. Ni was deposited onto the cleaved NaCl (001) substrates, which

were kept at 673 K during deposition. Subsequently, the substrates were cooled down to room temperature and C was deposited onto Ni, without exposing the specimens to air. The mean thicknesses of the deposited Ni and C layers were 0.8 and 10.0 nm, respectively. The specimens for TEM and Raman spectroscopy were prepared by dissolving the NaCl substrates in distilled water and picking up the as-deposited films onto molybdenum TEM grids. The structure of the specimens was observed by high-resolution TEM and electron diffraction. TEM imaging was carried out at an acceleration voltage of 120 kV. Raman spectra for the specimens were measured using a laser excitation source with a wavelength of 532 nm.

3. Results and Discussion

Figure 1(a) shows a low-magnification image of a carbon film deposited onto Ni at room temperature under ultrahigh vacuum. Ni forms isolated particles with an average size of 5.6 nm on the carbon film. The size distribution of the nanoparticles is shown in Fig. 2 and its standard deviation is 0.7 nm. Figure 1(b) shows a selected-area electron diffraction pattern taken from the specimen in Fig. 1(a). The electron diffraction pattern is composed of a halo pattern and single-crystalline spots. The halo pattern results from amorphous carbon and the spots are assigned to fcc-Ni with a zone axis of [001]. The Ni nanoparticles grown on the NaCl (001) substrate have an orientation relationship of $[100]_{Ni}$ // $[100]_{NaCl}$, $(001)_{Ni}$ // $(001)_{NaCl}$, as previously reported.[13] In Fig. 1(b), no nickel oxide and nickel carbide was observed. The profile of the Ni nanoparticles seen in Fig. 1(a) is a square. The square profile probably corresponds to a projected outline of a truncated octahedron with {111} and {100} facets seen along a [001] axis perpendicular to the nanoparticles, as reported about fcc-metal particles supported on NaCl and MgO substrates.[14,15]

Figure 3 shows a Raman spectrum measured for the specimen in Fig. 1, which is different from the Raman spectrum for a-C.[16] The broad spectrum peaks found in the

900-1800 cm^{-1} range are decomposed into those of the D and G modes which are related to the E_{2g} and disorder-induced modes on graphite, respectively.[17] In the present study, the Raman spectrum peaks were analyzed by two Gaussian fit. The peaks of the D and G modes appear at 1388 and 1582 cm^{-1}, respectively. The peak-intensity ratio of the D to G modes (I_D/I_G) is 1.5. The domain size of graphite L_a can be estimated using the Tuinstra-Koenig relation, La (nm) = $C(\lambda)[I_D/I_G]^{-1}$, where λ is a wavelength of a laser excitation source and C(532 nm) = 4.95 nm.[18] La in the present study was calculated to be 3.3 nm, which was smaller than the average size of the Ni nanoparticles. The present result indicates that the as-deposited a-C film contains nanometer-sized-crystalline graphite besides amorphous carbon.

In order to examine in detail the structure of the as-deposited a-C films on the clean surfaces of the Ni nanoparticles, we investigated the a-C films by high-resolution TEM. The high-resolution images of the a-C film on individual Ni nanoparticles in the specimen of Fig. 1 are shown in Figs. 4(a) and 4(b). The dark regions in the center of the images are the Ni nanoparticles and the sizes of the nanoparticles seen in Figs. 4(a) and 4(b) are 6.6 and 5.7 nm, respectively. It is noted that disordered graphitic layers are formed only around the Ni nanoparticles, as shown in Figs. 4(a) and 4(b), even though the a-C film was not annealed at all. The structure of the disordered graphitic layers is similar to that of carbon black.[19] Additionally, as for the a-C film deposited onto the Ni nanoparticles that were exposed to air once, the disordered graphitic layers were not formed around the nanoparticles. Since it is hard to distinguish the detail structure of the disordered graphitic layers from the high-resolution images in Figs. 4(a) and 4(b), a Fourier transformation analysis for these images was carried out. Filtered inverse fast Fourier transformed images of Figs. 4(a) and 4(b) are shown in Figs. 4(c) and 4(d), respectively, which were produced by applying an annular filter with a passband of 2 to 3 nm^{-1}. The Ni nanoparticles are clearly surrounded by the

disordered graphitic layers whose length approximately ranges from 3 to 5 nm. The order of the length of the disordered graphitic layers is consistent with that of L_a estimated from I_D/I_G for Raman spectrum in Fig. 3. The number of the layers is more than three. The spacing of the layers indicated by the arrows in Figs. 4(c) and 4(d) is about 0.37 and 0.39 nm, which is wider than that of graphite.

The graphitic-film formation by the reaction of transition metals, such as nickel, iron, and cobalt, with a-C have been studied and also used as a recent approach to synthesizing graphene.[8-12, 20-22] In the previous reports, the graphitization for a-C, caused by dissolution of carbon in metal at a high temperature and precipitation of graphitic carbon on the metal surface during cooling, did not observe unless the specimens were annealed at high temperature. On the other hand, in the present study, TEM and Raman spectroscopy observations show the formation of disordered graphitic carbon at room temperature on the surfaces of the Ni nanoparticles, which were not oxidized. The clean surfaces of the Ni nanoparticles may increase catalytic activity and reduce the graphenization temperature of a-C as a result of lattice softening arising from the large proportion of surface atoms to the whole in the nanoparticles.[23] However, there is also another possibility that the mechanism of graphitization in the present study is different from that in the previous reports, i.e., the direct growth of the disordered graphitic layers on the clean surfaces of the Ni nanoparticles occurs without passing through the process of dissolution and precipitation of carbon. The elucidation of the mechanism of graphitization of a-C on the clean surfaces of the Ni nanoparticles needs further studies.

4. Conclusion

We revealed that the a-C film deposited on the clean surfaces of the Ni nanoparticles at room temperature spontaneously formed several layers of disordered graphitic carbon

without heat treatment, suggesting that controlling the initial surface state of the catalytic metals, particularly the cleanliness of the catalytic metals plays an important role in the decrease in the metal-catalyzed graphitization temperature of a-C. The present study may lead to a new approach to fabricate graphitic nanomaterials such as graphene quantum dots.

Acknowledgments

This study was partly supported by a research granted from The Murata Science Foundation and Hosokawa Powder Technology Foundation.

References

[1] S. V. Morozov, K. S. Novoselov, M. I. Katsnelson, F. Schedin, D. C. Elias, J. A. Jaszczak, A. K. Geim, Phys. Rev. Lett. **2008**, *100*, 016602.

[2] K. I. Bolotin, K. J. Sikes, Z. Jiang , M. Klima, G. Fudenberg, J. Hone, P. Kim, H. L. Stormer , Solid State Commun. **2008**, *146*, 351.

[3] A. A. Balandin, S. Ghosh, W. Bao, I. Calizo, D. Teweldebrhan, F. Miao, C. N. Lau, Nano Lett. **2008**, *8*, 902.

[4] A. K. Geim, K. S. Novoselov, Nature Mater. **2005**, *6*, 183.

[5] C. Lee, X. D. Wei, J. W. Kysar, J. Hone, Science **2008**, *321*, 385.

[6] Y. Zhu, S. Murali, W. Cai, X. Li, J. W. Suk, J. R. Potts, R. S. Ruoff, Adv. Mater. **2010**, *22*, 3906.

[7] M. J. Allen, V. C. Tung, R. B. Kaner, Chem. Rev. **2010**, *110*, 132.

[8] M. Zheng, K. Takei, B. Hsia, H. Fang, X. Zhang, N. Ferralis, H. Ko, Y.-L. Chueh, Y. Zhang, R. Maboudian, A. Javey, Appl. Phys. Lett. **2010**, *96*, 063110.

[9] Z. Sun, Z. Yan, J. Yao, E. Beitler, Y. Zhu, J. M. Tour, Nature **2010**, *468*, 549.

[10] C. M. Orofeo, H. Ago, B. Hu, M. Tsuji, NanoRes. **2011**, *4*, 531.

[11] K. Wang, G. Tai, K. H. Wong, S. P. Lau, W. Guo, AIP Advances **2011**, *1*, 022141.

[12] K. Fujita, K. Banno, H. R. Aryal, T. Egawa, Appl. Phys. Lett. **2012**, *101*, 163109.

[13] S. Ino, D. Watanabe, S. Ogawa, J. Phys. Soc. Japan **1964**, *19*, 881

[14] K. Fukaya, S. Ino, S. Ogawa, Trans. JPN. Inst. Met. **1978**, *19*, 445.

[15] S. Giorgio, C.R. Henry, C. Chapon, J. M. Penisson, J. Cryst. Growth **1990**, *100*, 254.

[16] A. C. Ferrari, J. Robertson, Phys. Rev. B **2001**, *64*, 075414.

[17] S. Reich, C. Thomsen, Philos. Trans. R. Soc. Lond. A, **2004**, *362*, 2271.

[18] A. Ismach, C. Druzgalski, S. Penwell, A. Schwartzberg, M. Zheng, A. Javey, J. Bokor, Y. Zhang, Nano Lett. **2010**, *10*, 1542.

[19] R. D. Heidenreich, W. M. Hess, L. L. Ban, J. Appl. Cryst. **1968**, *1*, 1.

[20] F. J, Derbyshire, A. E. B. Presland, D. L. Trimm, Carbon **1972**, *10*, 114.

[21] F. J, Derbyshire, A. E. B. Presland, D. L. Trimm, Carbon **1975**, *13*, 111.

[22] R. Anton, Carbon **2008**, *46*, 656.

[23] J. Harada, K. Ohshima, Surf. Sci. **1981**, *106*, 51.

Figure captions

Fig. 1. (a) Low-magnification image and (b) selected-area electron diffraction pattern of an a-C film deposited onto Ni nanoparticles under ultrahigh vacuum. Spots in (b) are assigned to fcc-Ni with a zone axis of [001].

Fig. 2. Size distribution of the Ni nanoparticles in the specimen of Fig. 1 (a). The average size of the nanoparticles is 5.6 nm and the standard deviation is 0.7 nm.

Fig. 3. Raman spectrum of the specimen in Fig. 1. Curve fitting result is shown by a broken line. The D peak and G peak appear at 1388 and 1582 cm^{-1}, respectively.

Fig. 4. (a) and (b) High-resolution images of the a-C film around individual Ni nanoparticles. Disordered graphitic layers are formed only around the Ni nanoparticles, although the a-C film was not heat treated at all. (c) and (d) Filtered inverse fast Fourier transformed images of (a) and (b), respectively.

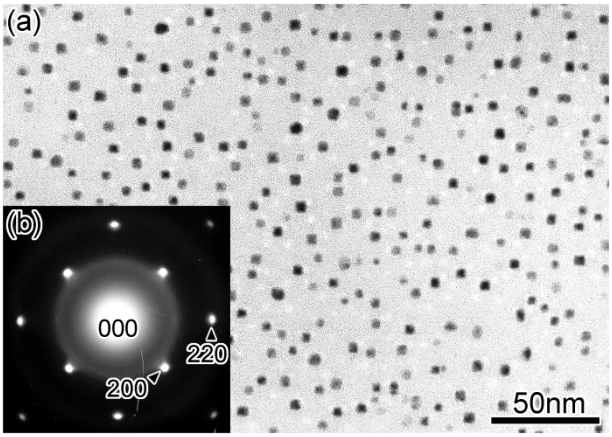

Fig. 1

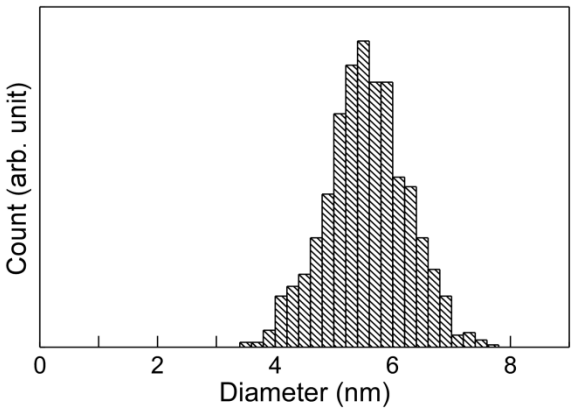

Fig. 2

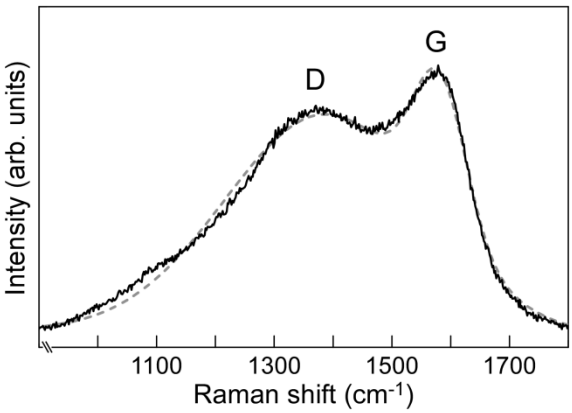

Fig. 3

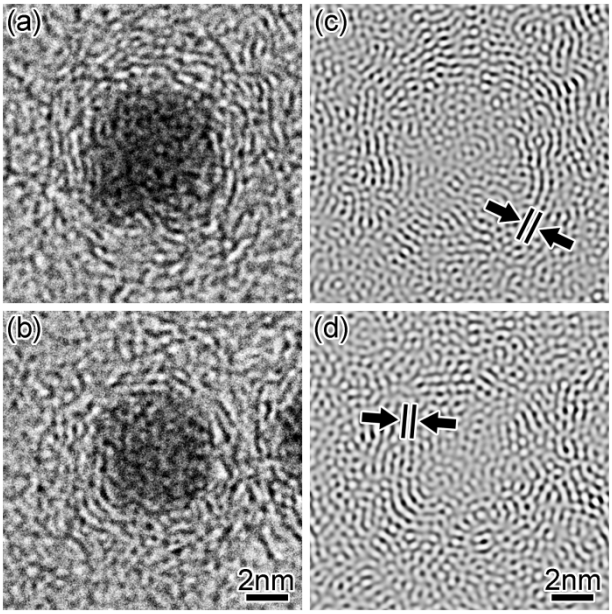

Fig. 4